**International Academy of Science,
Engineering and Technology**
Connecting Researchers; Nurturing Innovations
IASET

A NOVEL DIRECT POWER CONTROL METHOD OF MATRIX CONVERTER AS UPFC

T. VARA PRASAD[1] & GOWTHAM CHENDRA[2]

[1]Associate Professor, Department of Electrical and Electronics Engineering, S.V.P.C.E.T., Puttur, Andhra Pradesh, India

[2]PG Scholar, Department of Electrical and Electronics Engineering, S.V.P.C.E.T., Puttur, Andhra Pradesh, India

ABSTRACT

This paper presents state space vector analysis for three-phase matrix converter (MC) operating as unified power flow controllers (UPFCs). It allows direct ac/ac power conversion without dc energy storage links; therefore, it reduces volume, cost, and capacitor power losses, together with higher reliability. The line active and reactive power, together with ac supply reactive power, can be directly controlled by selecting an appropriate matrix converter switching state guaranteeing good steady-state and dynamic responses. This advanced control of MC guarantee faster responses without overshoot and no steady- state error, presenting no cross-coupling in dynamic and steady-state responses. Simulations are carried out, showing the effectiveness of the proposed method in steady-state and transient conditions.

KEYWORDS: Direct Power Control (DPC), Matrix Converter (MC), Unified Power Flow Controller (UPFC), State Space Vectors

INTRODUCTION

In the last few years Flexible AC Transmission Systems (FACTS) became well known power electronics based equipment to control transmission lines power flow. UPFCs are the most versatile and complex FACTS allowing precise and reliable control of both active and reactive power flow over the network. UPFC can prevail over line impedance dependencies, sending and receiving end voltage amplitudes and phase differences. The original UPFC concept, introduced in the nineties by L. Gyugyi[1], consists of two AC-DC converters using Gate- Turn Off thyristors(GTO), back to back connected through their common DC link using large high-voltage DC storage capacitors. Both converters AC *sides* are connected to the transmission line, through coupling transformers, in shunt and series connection with the line [2]-[8].

This arrangement can be operated as an ideal reversible AC-AC switching power converter, in which the power can flow in either direction between the AC terminals of the two converters. The DC link capacitors provide some energy storage capability to the back to back converters that help the power flow control Replacing the two three-phase inverters by one matrix converter the DC link(bulk) capacitors are eliminated, reducing costs, size, maintenance, increasing reliability and lifetime. The AC-AC matrix converter, also known as all silicon converters, processes the energy directly without large energy storage needs. This leads to an increase of the matrix converter control complexity. In [9] an UPFC-connected power transmission network model was proposed with matrix converters and in [10]- [12] was used to synthesize both active (P) and reactive (Q) power controllers using a modified venturini high-frequency PWM modulator[11].

In the last few years direct power control techniques have been used in many power applications, due to their simplicity and good performance [14]-[17]. In this paper a Matrix Converter based UPFC-connected power transmission network model is proposed, using a Direct Power Control approach (DPC-MC). This control method is based on sliding mode control techniques [20]-[22] and allows real time selection of adequate state-space vectors to control input and

output variables [7]. Transmission line active and reactive power flow can be directly controlled using this approach and the dynamic and steady state behavior of the proposed P, Q control method is evaluated and discussed using detailed simulations. Results shows decoupled active and reactive power control, zero error tracking and fast response times.

MODELLING OF THE UPFC POWER SYSTEM

General Architecture

A simplified power transmission network using the proposed matrix converter UPFC is presented in Figure 1, where V_S and V_R are, respectively, the sending-end and receiving-end sinusoidal voltages of the Z_S and Z_R generators feeding load Z_L. The matrix converter is connected to transmission line 2, represented as a series inductance with series resistance (L_2 and R_2), through coupling transformers T_1 and T_2.
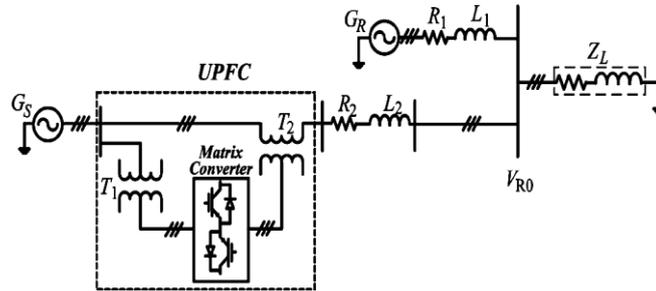

Figure 1: Transmission Network with Matrix Converter UPFC

Figure 2 shows the simplified three-phase equivalent circuit of the matrix UPFC transmission system model. For system modeling, the power sources and the coupling transformers are all considered ideal. Also, the matrix converter is considered ideal and represented as a controllable voltage source, with amplitude V_C and phase ρ. In the equivalent circuit, V_{RO} is the load bus voltage. The DPC-MC controller will treat the simplified elements as disturbances.

Considering a symmetrical and balanced three-phase system and applying Kirchhoff laws to the three-phase equivalent circuit (Figure 2), the ac line currents are obtained in *dq* coordinates as (1) and (2) equations
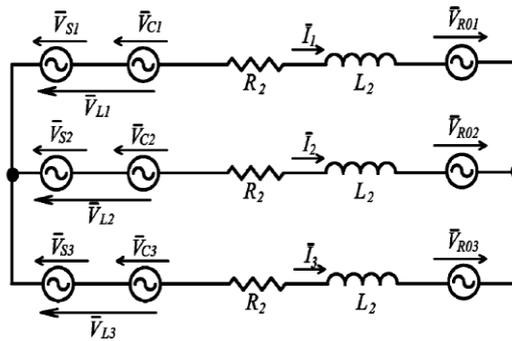

Figure 2: Three Phase Equivalent Circuit of the Matrix UPFC and Transmission Line

$$\frac{dI_d}{dt} = \omega I_q - \frac{R_2}{L_2} I_d + \frac{1}{L_2}(V_{Ld} - V_{Rod}) \tag{1}$$

$$\frac{dI_q}{dt} = -\omega I_d - \frac{R_2}{L_2} I_q + \frac{1}{L_2}(V_{Lq} - V_{Roq}) \tag{2}$$

The active and reactive power of sending end generator are given in *dq* coordinates

$$\begin{bmatrix} P \\ Q \end{bmatrix} = \begin{bmatrix} V_d & V_q \\ v_q & -V_d \end{bmatrix} \begin{bmatrix} I_d \\ I_q \end{bmatrix} \tag{3}$$

Assuming V_{ROd} and $V_{Sd} = V_d$ as constants and a rotating reference frame synchronised to the Vs source so that $V_{Sq} = 0$, active and reactive power P and Q are given by (4) and (5), respectively.

$$P = V_d I_d \tag{4}$$

$$Q = -V_d I_q \tag{5}$$

Based on the desired active and reactive power (P_{ref}, Q_{ref}), reference current (I_{dref}, I_{qref}) can be calculated from (4) and (5) for current controllers. However, allowing P, Q actual powers are sensitive to errors in the V_d, V_q values.

Matrix Converter Output Voltage and Input Current Vectors

A diagram of UPFC system (Figure 3) includes the three-phase shunt input transformer (with windings T_a, T_b, T_c), the three-phase series output transformer (with windings T_A, T_B, T_C), and the three-phase matrix converter, represented as an array of nine bidirectional switches S_{kj} with turn-on and turn-off capability, allowing the connection of each one of three output phases directly to any one of the three input phases. The three-phase (*lCr*) input filter is required to re-establish a voltage-source boundary to the matrix converter, enabling smooth input currents.

Applying coordinates to the input filter state variables presented in Figure 3 and neglecting the effects of the damping resistors, the following equations are obtained.
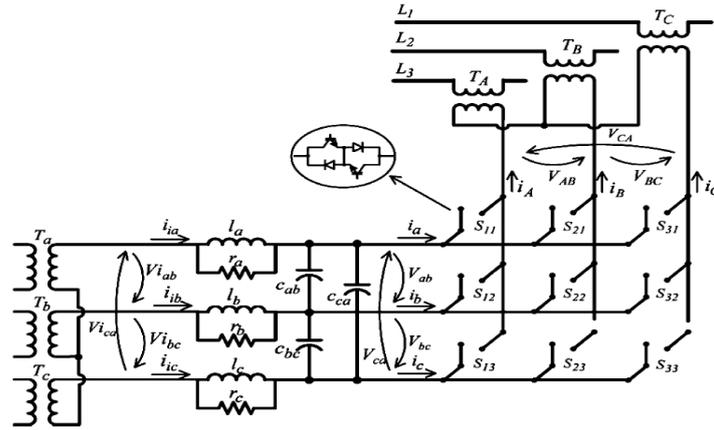

Figure 3: Transmission Network with Matrix Converter UPFC

$$\frac{di_{id}}{dt} = \omega i_{iq} - \frac{1}{2l}V_d - \frac{1}{2\sqrt{3}l}V_q + \frac{1}{l}V_{id}$$

$$\frac{di_{id}}{dt} = -\omega i_{id} - \frac{1}{2l}V_q + \frac{1}{2\sqrt{3}l}V_d + \frac{1}{l}V_{iq}$$

$$\frac{dV_d}{dt} = \omega V_q - \frac{1}{2\sqrt{3}C}i_{iq} + \frac{1}{2C}i_{id} - \frac{1}{2C}i_d + \frac{1}{2\sqrt{3}C}i_q \tag{6}$$

$$\frac{dV_q}{dt} = -\omega V_d + \frac{1}{2\sqrt{3}C}i_{id} + \frac{1}{2C}i_{iq} - \frac{1}{2C}i_q - \frac{1}{2\sqrt{3}C}i_d$$

Where V_{id}, V_{iq}, i_{id}, i_{iq} represent, respectively, input voltages and input currents in *dq* components (at the shunt transformer secondary) and V_d, V_q, i_d, i_q are the matrix converter voltages and input currents in components, respectively.

Assuming ideal semiconductors, each matrix converter bidirectional switch can assume two possible states: "$S_{kj}=1$" if the switch is closed or "$S_{kj}=0$" if the switch is open. The nine matrix converter switches can be represented as

$$S = \begin{bmatrix} S_{11} & S_{12} & S_{13} \\ S_{21} & S_{22} & S_{23} \\ S_{31} & S_{32} & S_{33} \end{bmatrix} \tag{7}$$

The matrix converter topological constraints imply $\sum_{j=1}^{3} S_{kj} = 1$.

Based on (7), the relationship between load and input voltages can be expressed as

$$[v_A \quad v_B \quad v_C]^T = S[v_a \quad v_b \quad v_c]^T \tag{8}$$

The input phase current can be related to the output phase currents (9), using the transpose of matrix S

$$[i_a \quad i_b \quad i_c]^T = S^T[i_A \quad i_B \quad i_C]^T \tag{9}$$

From the 27 possible switching patterns, time-variant vectors can be obtained (Table:1) representing the matrix output voltages and input currents in αβ frame [figure 4(b)].

The active and reactive power DPC-MC will select one of these 27 vectors at any given time instant.

DIRECT POWER CONTROL OF MC-UPFC

Line Active and Reactive Power Sliding Surfaces

The DPC controllers for line power flow are here derived based on the sliding mode control theory.

From Figure 2, in steady state, V_d is imposed by source Vs. From (1) and (2),the transmission-line current can be considered as state variables with first-order dynamics dependent on the sources and time constant of impedance L_2/R_2. Therefore, transmission-line active and reactive powers present first-order dynamics and have a strong relative degree of one [18], since from the control view point; its first time derivative already contains the control variable [19]-[22]. From the sliding mode control theory, robust sliding surfaces to control the P and Q variables with a relatively strong degree of one can be obtain, considering proportionality to a linear combination of the errors of the state variables.

Therefore define the active power error e_P and the reactive power e_Q as the difference between the power references P_{ref},Q_{ref} and the actual transmitted powers P,Q respectively

$$e_P = P_{ref} - P \tag{10}$$

$$e_Q = Q_{ref} - Q \tag{11}$$

Then the sliding surfaces $S_P(e_P,t)$ and $S_Q(e_Q,t)$ must be proportional to these errors, being zero after reaching sliding mode

$$S_P(e_P, t) = k_P(P_{ref} - P) \tag{12}$$

$$S_Q(e_Q, t) = k_Q(Q_{ref} - Q) \tag{13}$$

The proportionality gains k_P and k_Q are chosen to impose appropriate switching frequencies.

Line Active and Reactive Power Direct Switching Laws

Based on errors e_P and e_Q to select in real time the matrix converter switching states. To guarantee stability for active power and reactive power controllers the sliding mode stability conditions (14) and (15) must be verified.

$$S_P(e_P, t)\dot{S}_P(e_P, t) < 0 \tag{14}$$

$$S_Q(e_Q, t)\dot{S}_Q(e_Q, t) < 0 \tag{15}$$

These conditions mean that if $S_P(e_P, t) > 0$, then the $S_P(e_P, t)$ value must be decreased, meaning that its time derivative should be negative $(\dot{S}_P(e_P, t) < 0)$. Similarly if $S_P(e_P, t) < 0$, then $\dot{S}_P(e_P, t) > 0$.

According to (12) and (14), the criteria to choose the matrix vector should be:

- $S_P(e_P, t) > 0 \Rightarrow \dot{S}_P(e_P, t) < 0 \Rightarrow$ P<P_{ref},

  Then choose a vector suitable to increase P.

- $S_P(e_P, t) < 0 \Rightarrow \dot{S}_P(e_P, t) > 0 \Rightarrow$ P>P_{ref},

  Then choose a vector suitable to decrease P.

- If $S_P(e_P, t) = 0$

  Then choose a vector which does not significantly change the active power.   (16)

  The same can be applied to reactive power error.

a) To choose a vector from (4) and (12), and considering P_{ref} and V_d in steady state, the following can be written:

$$\dot{S}_P(e_P, t) = K_P \left(\frac{dP_{ref}}{dt} - \frac{dP}{dt} \right) = -K_P \frac{dP}{dt} = -K_P \frac{d(V_d I_d)}{dt} = -K_P V_d \frac{dI_d}{dt} \qquad (17)$$
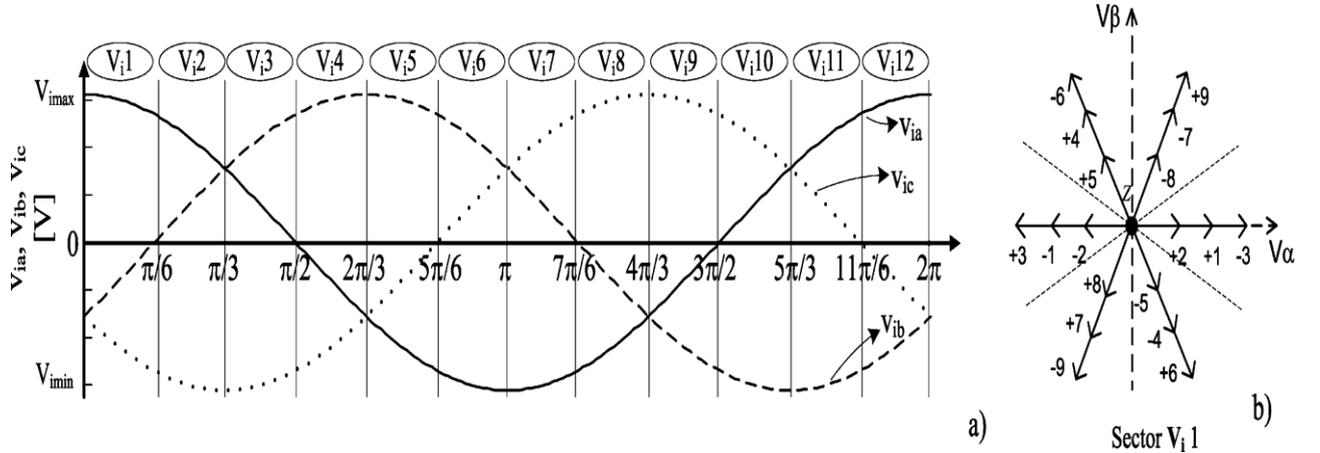

Figure 4: (a) Input Voltages and their Corresponding Sector. (b)Output Voltage State Space Vectors when the Input Voltages a Relocated at Sector V_i1

Considering V_d and P_{ref} as constant if $S_P(e_P, t) > 0$, then it must be $\dot{S}_P(e_P, t) < 0$. From (16) if $K_P V_d$ is positive, then $dI_d/dt > 0$, meaning that P must increase.

From the equivalent model in *dq* coordinates in (1) if the chosen vector has $V_{Ld} > V_{Rod} - \omega I_q L_2 + R_2 I_d$ then $dI_d/dt > 0$,the selected vector being suitable to increase the active power.

b) Similarly from (5) and (13) with reactive power Q_{ref} and V_d in steady state

$$\dot{S}_Q(e_Q, t) = K_Q \left(\frac{dQ_{ref}}{dt} - \frac{dQ}{dt} \right) = -K_P \frac{dQ}{dt} = -K_Q \frac{d(-V_d I_q)}{dt} = K_Q V_d \frac{dI_q}{dt} \qquad (18)$$

Table 1: Switching Combinations and Output Voltage/Input Current State-Space Vectors

Group	Name	A	B	C	v_{AB}	v_{BC}	v_{CA}	i_a	i_b	i_c	V_o	δ_o	I_i	μ_i
	1g	a	b	c	v_{ab}	v_{bc}	v_{ca}	i_A	i_B	i_C	v_i	δ_i	$\sqrt{3}i_o$	μ_o
	2g	a	c	b	$-v_{ca}$	$-v_{bc}$	$-v_{ab}$	i_A	i_C	i_B	$-v_i$	$-\delta_i+4\pi/3$	$\sqrt{3}i_o$	$-\mu_o$
I	3g	b	a	c	$-v_{ab}$	$-v_{ca}$	$-v_{bc}$	i_B	i_A	i_C	$-v_i$	δ_i	$\sqrt{3}i_o$	$-\mu_o+2\pi/3$
	4g	b	c	a	v_{bc}	v_{ca}	v_{ab}	i_C	i_A	i_B	v_i	$\delta_i+4\pi/3$	$\sqrt{3}i_o$	$\mu_o+2\pi/3$
	5g	c	a	b	v_{ca}	v_{ab}	v_{bc}	i_B	i_C	i_A	v_i	$\delta_i+2\pi/3$	$\sqrt{3}i_o$	$\mu_o+4\pi/3$
	6g	c	b	a	$-v_{bc}$	$-v_{ab}$	$-v_{ca}$	i_C	i_B	i_A	$-v_i$	$-\delta_i+2\pi/3$	$\sqrt{3}i_o$	$-\mu_o+4\pi/3$
	+1	a	b	b	v_{ab}	0	$-v_{ab}$	i_A	$-i_A$	0	$\sqrt{2/3}v_{ab}$	0	$\sqrt{2}i_A$	$-\pi/6$
	-1	b	a	a	$-v_{ab}$	0	v_{ab}	$-i_A$	i_A	0	$-\sqrt{2/3}v_{ab}$	0	$-\sqrt{2}i_A$	$-\pi/6$
	+2	b	c	c	v_{bc}	0	$-v_{bc}$	0	i_A	$-i_A$	$\sqrt{2/3}v_{bc}$	0	$\sqrt{2}i_A$	$\pi/2$
	-2	c	b	b	$-v_{bc}$	0	v_{bc}	0	$-i_A$	i_A	$-\sqrt{2/3}v_{bc}$	0	$-\sqrt{2}i_A$	$\pi/2$
	+3	c	a	a	v_{ca}	0	$-v_{ca}$	$-i_A$	0	i_A	$\sqrt{2/3}v_{ca}$	0	$\sqrt{2}i_A$	$7\pi/6$
	-3	a	c	c	$-v_{ca}$	0	v_{ca}	i_A	0	$-i_A$	$-\sqrt{2/3}v_{ca}$	0	$-\sqrt{2}i_A$	$7\pi/6$
	+4	b	a	b	$-v_{ab}$	v_{ab}	0	i_B	$-i_B$	0	$\sqrt{2/3}v_{ab}$	$2\pi/3$	$\sqrt{2}i_B$	$-\pi/6$
	-4	a	b	a	v_{ab}	$-v_{ab}$	0	$-i_B$	i_B	0	$-\sqrt{2/3}v_{ab}$	$2\pi/3$	$-\sqrt{2}i_B$	$-\pi/6$
II	+5	c	b	c	$-v_{bc}$	v_{bc}	0	0	i_B	$-i_B$	$\sqrt{2/3}v_{bc}$	$2\pi/3$	$\sqrt{2}i_B$	$\pi/2$
	-5	b	c	b	v_{bc}	$-v_{bc}$	0	0	$-i_B$	i_B	$-\sqrt{2/3}v_{bc}$	$2\pi/3$	$-\sqrt{2}i_B$	$\pi/2$
	+6	a	c	a	$-v_{ca}$	v_{ca}	0	$-i_B$	0	i_B	$\sqrt{2/3}v_{ca}$	$2\pi/3$	$\sqrt{2}i_B$	$7\pi/6$
	-6	c	a	c	v_{ca}	$-v_{ca}$	0	i_B	0	$-i_B$	$-\sqrt{2/3}v_{ca}$	$2\pi/3$	$-\sqrt{2}i_B$	$7\pi/6$
	+7	b	b	a	0	$-v_{ab}$	v_{ab}	i_C	$-i_C$	0	$\sqrt{2/3}v_{ab}$	$4\pi/3$	$\sqrt{2}i_C$	$-\pi/6$
	-7	a	a	b	0	v_{ab}	$-v_{ab}$	$-i_C$	i_C	0	$-\sqrt{2/3}v_{ab}$	$4\pi/3$	$-\sqrt{2}i_C$	$-\pi/6$
	+8	c	c	b	0	$-v_{bc}$	v_{bc}	0	i_C	$-i_C$	$\sqrt{2/3}v_{bc}$	$4\pi/3$	$\sqrt{2}i_C$	$\pi/2$
	-8	b	b	c	0	v_{bc}	$-v_{bc}$	0	$-i_C$	i_C	$-\sqrt{2/3}v_{bc}$	$4\pi/3$	$-\sqrt{2}i_C$	$\pi/2$
	+9	a	a	c	0	$-v_{ca}$	v_{ca}	$-i_C$	0	i_C	$\sqrt{2/3}v_{ca}$	$4\pi/3$	$\sqrt{2}i_C$	$7\pi/6$
	-9	c	c	a	0	v_{ca}	$-v_{ca}$	i_C	0	$-i_C$	$-\sqrt{2/3}v_{ca}$	$4\pi/3$	$-\sqrt{2}i_C$	$7\pi/6$
	z_a	a	a	a	0	0	0	0	0	0	0	-	0	-
III	z_b	b	b	b	0	0	0	0	0	0	0	-	0	-
	z_c	c	c	c	0	0	0	0	0	0	0	-	0	-

If $S_Q(e_Q, t) > 0$, then $\dot{S}_Q(e_Q, t) < 0$ which still implies dQ/dt>0, meaning that Q must increase. From (18) dIq/dt must be negative from the equivalent model in dq coordinates in (2) to ensure the reaching condition, the chosen vector has $V_{Lq} < V_{Roq} + \omega I_d L_2 + R_2 I_q$ to guarantee $dI_q/dt < 0$, meaning the voltage vector has q component suitable to increase the reactive power.

To ease vector selection (Table 1), sliding surfaces $S_P(e_P, t)$ and $S_Q(e_Q, t)$ should be transformed to $\alpha\beta$ coordinates $S_\alpha(e_P, t)$, $S_\beta(e_Q, t)$.

To design the DPC control system, the six vectors of group I will not be used, since they require extra algorithms to calculate their time-varying phase [13]. From group II, the variable amplitude vectors, only the 12 highest amplitude voltage vectors are certain to be able to guarantee the previously discussed required levels of V_{Ld} and V_{Lq} needed to fulfill the reaching conditions. The lowest amplitude voltages vectors, or the three null vectors of group III, could be used for near zero errors.

If the control errors e_P and e_Q are quantized using two hysteresis comparators, each with three levels (-1, 0 and +1), nine output voltage error combinations are obtained. If a two-level comparator is used to control the shunt reactive power, as discussed in next subsection, 18 error combinations(9x2=18) will be defined, enabling the selection of 18 vectors. Since the three zero vectors have a minor influence on the shunt reactive power control, selecting one out 18 vectors is adequate.

As an example, consider the case of $C_\alpha = S_\alpha(e_P, t) > 0$ and $C_\beta = S_\beta(e_Q, t) < 0$. Then, dP/dt>0 and dQ/dt<0 imply that $dI_\alpha/dt>0$ and $dI_\beta/dt<0$. According to Table 1, output voltage vectors depend on the input voltages (sending voltage), so to choose the adequate output voltage vector, it is necessary to know the input voltages location [Fig.ure 4(a)]. Suppose now that the input voltages are in sector V_i1 [Figure 4(b)], then the vector to be applied should be +9 or -7. The final choice between these two depends on the matrix reactive power controller result C_{Qi}, discussed in the next subsection.

Table 2: State-Space Vectors Selection for Different Error Combinations

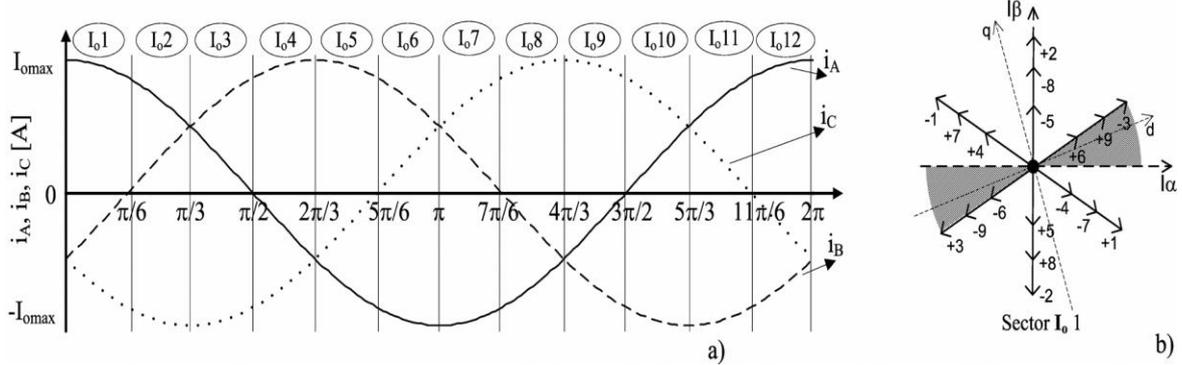| C_α	C_β	Sector					
		V_i 12; 1	V_i 2; 3	V_i 4; 5	V_i 6; 7	V_i 8; 9	V_i 10; 11
-1	+1	-9; +7	-9; +8	+8; -7	-7; +9	+9; -8	-8; +7
-1	0	+3; -1	+3; -2	-2; +1	+1; -3	-3; +2	+2; -1
-1	-1	-6; +4	-6; +5	+5; -4	-4; +6	+6; -5	-5; +4
0	+1	-9; +7; +6; -4	-9; +8; +6; -5	+8; -7; -5; +4	-7; +9; +4; -6	+9; -8; -6; +5	-8; +7; +5; -4
0	0	Za; Zb; Zc; -8;+2;-5;+8;-2;+5	Za; Zb; Zc; -7;+1;-4; +7;-1;+4	Za; Zb; Zc; +9;-3;+6;-9;+3;-6	Za; Zb; Zc; -8;+2;-5;+8;-2;+5	Za; Zb; Zc; -7;+1;-4; +7;-1;+4	Za; Zb; Zc; -9;+3;-6; +9;-3;+6
0	-1	-6; +4; +9; -7	+5; -6; -8; +9	+5; -4; -8; +7	-4; +6; +7; -9	+6; -5; -9; +8	-5; +4; +8; -7
+1	+1	+6; -4	+6; -5	-5; +4	+4; -6	-6; +5	+5; -4
+1	0	-3; +1	+2; -3	-1; +2	+3; -1	-2; +3	+1; -2
+1	-1	+9; -7	+9; -8	+7; -8	+7; -9	-9; +8	+8; -7

Figure 5: (a) Output Currents and their Corresponding Sector. (b) Input Current State-Space Vectors, when Output Currents a Relocated at Sector I_01. The *dq* Axis is Represented, Considering that the Input Voltages are Located in Zone V_i1

Using the same reasoning for the remaining eight active and reactive power error combinations and generalizing it for all other input voltage sectors, Table 2 is obtained. These P, Q controllers were designed based on control laws not dependent on system parameters, but only on the errors of the controlled output to ensure robustness to parameter variations or operating conditions and allow system order reduction, minimizing response times [26].

Direct Control of Matrix Converters Input Reactive Power

In addition, the matrix converter UPFC can be controlled to ensure a minimum or a certain desired reactive power at the matrix converter input. Similar to the previous considerations, since the voltage source input filter (Figure 3) dynamics (6) has a strong relative degree of two [25], then a suitable sliding surface $S_{Qi}(e_{Qi},t)$ (19) will be a linear combination of the desired reactive power error $e_{Qi}=Q_{iref}-Q_i$ and its first-order time derivative [29].

$$S_{Qi}(e_{Qi},t) = (Q_{iref} - Q_i) + k_{Qi}\frac{d}{dt}(Q_{iref} - Q_i) \tag{19}$$

The time derivative can be approximated by a discrete time difference, as k_{Qi} has been chosen to obtain a suitable switching frequency, since as stated before, this sliding surface needs to be quantized only in two levels (-1 and +1) using one hysteresis comparator.

To fulfill a stability condition similar to (15), considering the input filter dynamics (6), (20) is obtained

$$\dot{S}_{Qi}(e_{Qi}, t) = V_{id}\left(\frac{di_{iq}}{dt} + K_{Qi}\frac{d^2 i_{iq}}{dt^2}\right)$$

$$= V_{id}\left(-\omega i_{id} + \frac{1}{2\sqrt{3}l}V_d - \frac{1}{2l}V_q\right) + V_{id}K_{Qi}\left(-\omega^2 i_{iq} + \frac{\omega}{l}V_d + \frac{\omega}{\sqrt{3}l}V_q - \frac{\omega}{l}V_{id} - \frac{i_{iq}}{3lC} + \frac{i_q}{3lC}\right) \tag{20}$$

From (20), it is seen that the control input, the i_q matrix input current, must have enough amplitude to impose the sign of $\dot{S}_{Qi}(e_{Qi}, t)$ Supposing that there is enough i_q amplitude, (19) and (20) are used to establish the criteria (21) to choose the adequate matrix input current vector that imposes the needed sign of the matrix input-phase current i_q related to the output-phase currents by (9).

- $S_{Qi}(e_{Qi}, t) > 0 \Rightarrow \dot{S}_{Qi}(e_{Qi}, t) < 0$, then choose a vector with current $i_q < 0$ to increase Q_i.

- $S_{Qi}(e_{Qi}, t) < 0 \Rightarrow \dot{S}_{Qi}(e_{Qi}, t) > 0$ then choose a vector with current $i_q < 0$ to increase Q_i.   (21)

The sliding mode is reached when vectors applied to the converter have the necessary i_q current amplitude to satisfy stability conditions, such as (15). Therefore, to choose the most adequate vector in the chosen *dq* reference frame, it is necessary to know the output currents location since the i_q input current depends on the output currents (Table 1). Considering that the *dq*–axis location is synchronous with the v_{ia} input voltage (i.e., *dq* reference frame depends on the v_{ia} input voltage location), the sign of the matrix reactive power Q_i can be determined by knowing the location of the input voltages and the location of the output currents (Figure 5).

Considering the previous example, with the input voltage at sector V_i1 and sliding surfaces signals $S_\alpha(e_P, t) > 0$ and $S_\beta(e_Q, t) < 0$, both vectors +9 or -7 would be suitable to control the line active and reactive powers errors (Figure 4). However, at sector I_o1, these vectors have a different effect on the $\dot{S}_{Qi}(e_{Qi}, t)$ value: if i_q has suitable amplitude, vector +9 leads to $\dot{S}_{Qi}(e_{Qi}, t) > 0$ while vector -7 originates $\dot{S}_{Qi}(e_{Qi}, t) < 0$. So, vector +9 should be chosen if the input reactive power sliding surface $S_{Qi}(e_{Qi}, t)$ is quantized as $C_{Qi} = -1$, while vector -7 should be chosen when $S_{Qi}(e_{Qi}, t)$ is quantized as $C_{Qi} = +1$.

When the active and reactive power errors are quantized as zero, $S_\alpha(e_P, t) = 0$ and $S_\beta(e_Q, t) = 0$, the null vectors of group III, or the lowest amplitude voltages vectors at sector $V_i1(-8, +2, -5, +8, -2, +5)$ at Figure 4(b) could be used. These vectors do not produce significant effects on the line active and reactive power values, but the lowest amplitude voltage vectors have a high influence on the control of matrix reactive power. From Figure 5(b), only the highest amplitude current vectors of sector I_o1 should be chosen: vector +2 if $S_{Qi}(e_{Qi}, t)$ is quantized as $C_{Qi} = -1$, or vector -2 if $S_{Qi}(e_{Qi}, t)$ is quantized as $C_{Qi} = +1$.

Table 3: State Space Vector Selection for Output Currents Located at Sector V_i1

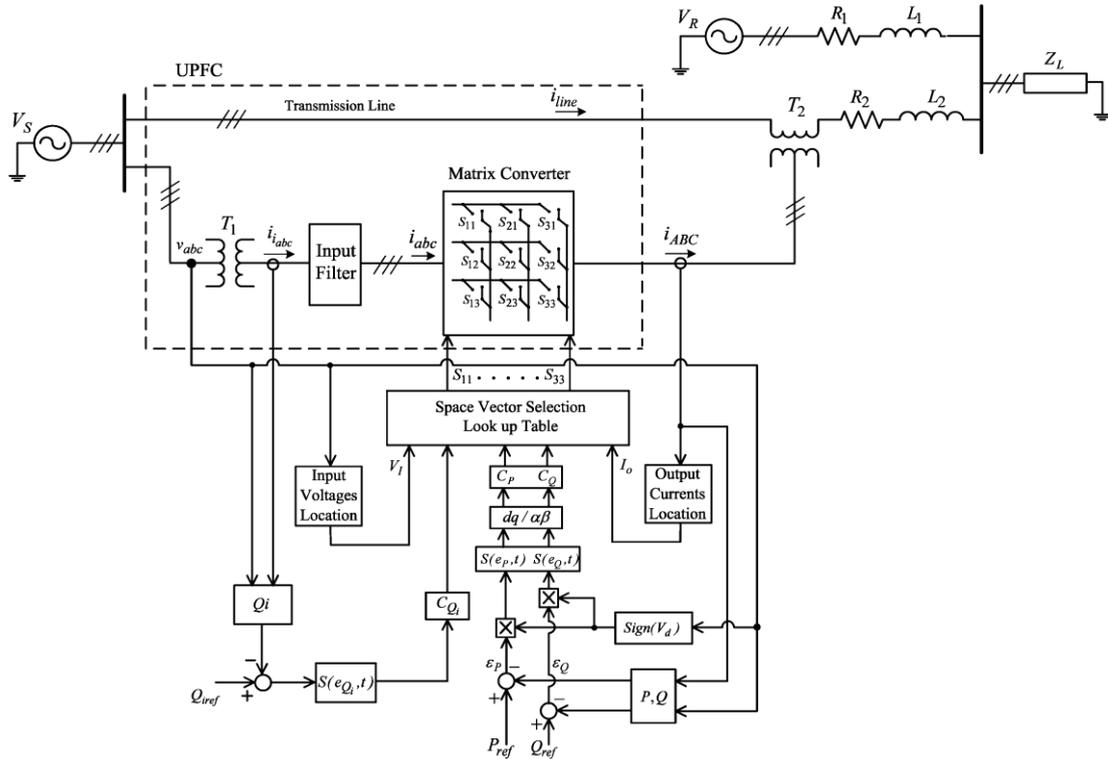| C_α | C_β | Sector |
|---|---|---|---|---|---|---|---|---|---|---|---|---|---|
| | | $I_o12 ; I_o1$ C_{Qi} | | $I_o2 ; I_o3$ C_{Qi} | | $I_o4 ; I_o5$ C_{Qi} | | $I_o6 ; I_o7$ C_{Qi} | | $I_o8 ; I_o9$ C_{Qi} | | $I_o10; I_o11$ C_{Qi} | |
| | | +1 | -1 | +1 | -1 | +1 | -1 | +1 | -1 | +1 | -1 | +1 | -1 |
| -1 | +1 | -9 | +7 | -9 | +7 | -9 | +7 | +7 | -9 | +7 | -9 | +7 | -9 |
| -1 | 0 | +3 | -1 | +3 | -1 | -1 | +3 | -1 | +3 | -1 | +3 | +3 | -1 |
| -1 | -1 | -6 | +4 | +4 | -6 | +4 | -6 | +4 | -6 | -6 | +4 | -6 | +4 |
| 0 | +1 | -9 | +7 | -9 | +7 | -9 | +7 | +7 | -9 | +7 | -9 | +7 | -9 |
| 0 | 0 | -2 | +2 | +8 | -8 | -5 | +5 | +2 | -2 | -8 | +8 | +5 | -5 |
| 0 | -1 | -7 | +9 | -7 | +9 | -7 | +9 | +9 | -7 | +9 | -7 | +9 | -7 |
| +1 | +1 | -4 | +6 | +6 | -4 | +6 | -4 | +6 | -4 | -4 | +6 | -4 | +6 |
| +1 | 0 | +1 | -3 | +1 | -3 | -3 | +1 | -3 | +1 | -3 | +1 | +1 | -3 |
| +1 | -1 | -7 | +9 | -7 | +9 | -7 | +9 | +9 | -7 | +9 | -7 | +9 | -7 |

Figure 6: Control Scheme of Direct Power Control of the Three-Phase Matrix Converter Operating as a UPFC

Using the same reasoning for the remaining eight combinations at sector V_i1 and applying it for the other output current sectors, Table 3 is obtained.

IMPLEMENTATION OF THE DPC-MC AS UPFC

As shown in the block diagram (Figure 6), the control of the instantaneous active and reactive powers requires the measurement of G_S voltages and output currents necessary to calculate $S_\alpha(e_P,t)$ and $S_\beta(e_Q,t)$ sliding surfaces. The output currents measurement is also used to determine the location of the input currents q component.

The control of the matrix converter input reactive power requires the input currents measurement to calculate $S_{Qi}(e_{Qi,}t)$.

At each time instant, the most suitable matrix vector is chosen upon the discrete values of the sliding surfaces, using tables derived from Tables 2 and 3 for all voltage sectors.

SIMULATION RESULTS

The performance of the proposed direct control system was evaluated with a detailed simulation model using the MATLAB to represent the matrix converter, transformers, sources and transmission lines, and Simulink blocks to simulate the control system. Ideal switches were considered to simulate matrix converter semiconductors minimizing simulation times.

The second-order input filter is l= 4.2 mH, C= 6.6 μF, r=25Ω. The load power is 1.5kW(1 p.u.) and transmission lines 1 and 2 are simulated as inductances L_1=12mH, L_2=15 mH, and series resistances R_1=R_2=0.2Ω, respectively for line 1 and 2. Sliding mode DPC gains are k_P=k_Q=k_{Qi}=1.
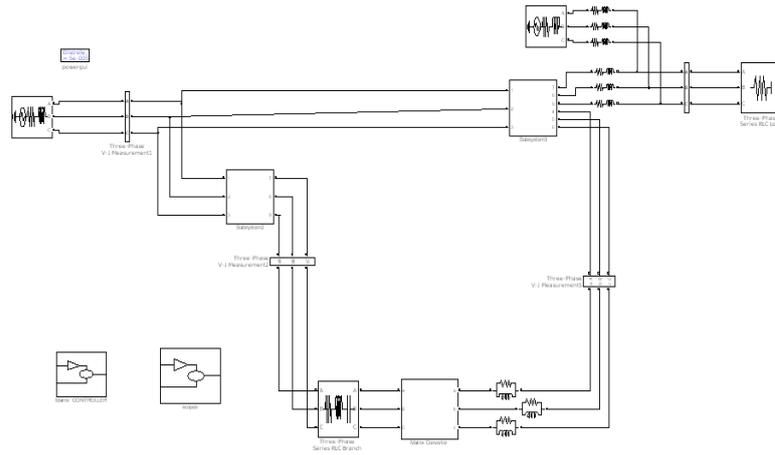
Figure 7: Transmission Network with Matrix Converter – UPFC

Figure 7 shows the simulation diagram of transmission matrix converter as UPFC using DPC method.

The simulation is operated for the step responses of active and reactive power references. For the simulation
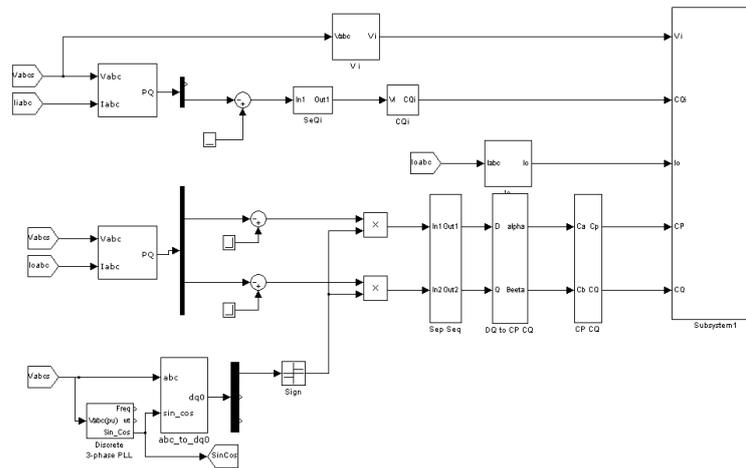

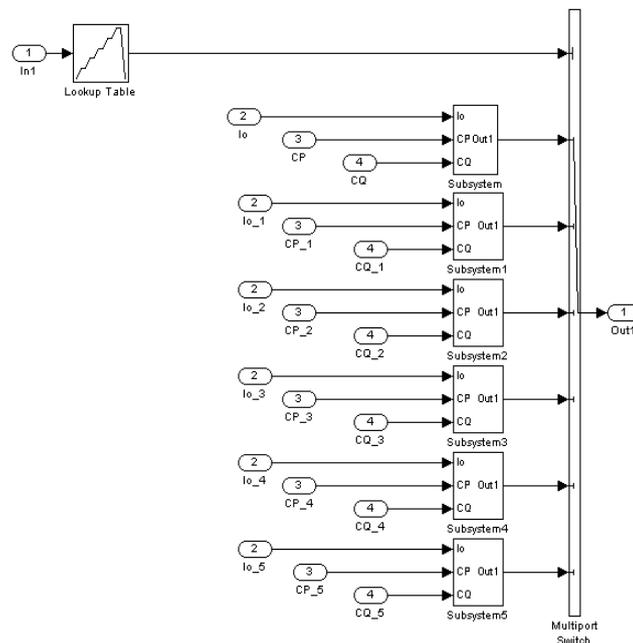**Figure 8: Control Scheme of Matrix Converter as UPFC Using Space Vector Selection Table**
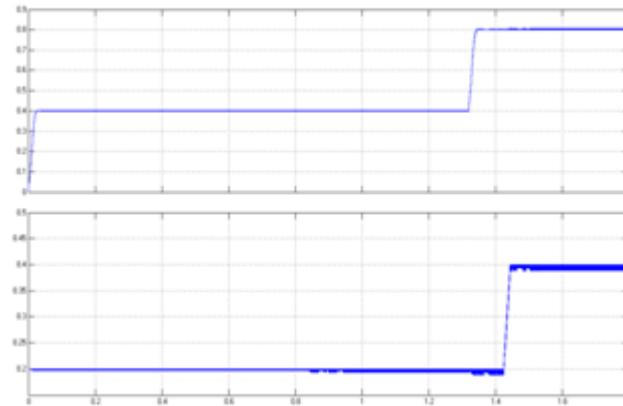

Figure 9: State Space Vector Selection

**Figure 10: Active and Reactive Series Power Response and Reactive
Shunt Power, for P and Q Steps (ΔP_{ref} =+0.4p.u.and ΔQ_{ref}=+0.2p.u.)**

Figure 10 shows the simulation results of the active and reactive power with step response (ΔP_{ref} =+0.4p.u.and ΔQ_{ref}=+0.2p.u.). Considering initial reference values: P_{ref}=0.4p.u. Q_{ref} =0.2p.u., and Q_{iref}=-0.07p.u. Both results clearly show that there is no cross-coupling between active and reactive power.

DPC controller ability to operate at lower switching frequencies, the DPC gains were lowered and the input filter parameters were changed accordingly (r=25Ω, l=5.9mH and C=12.6μF) to lower the switching frequencytonearly1.4kHz. The results (Figure 10) also show fast response without cross coupling between active and reactive power. This confirms the DPC-MC robustness to input filter parameter variation, the ability to operate at low switching frequencies, and insensitivity to Switching nonlinearity.

Figure 11 shows the simulation results of line currents for active and reactive power step changes and also it showing the claimed DPC faster response to step active and reactive power reference change.
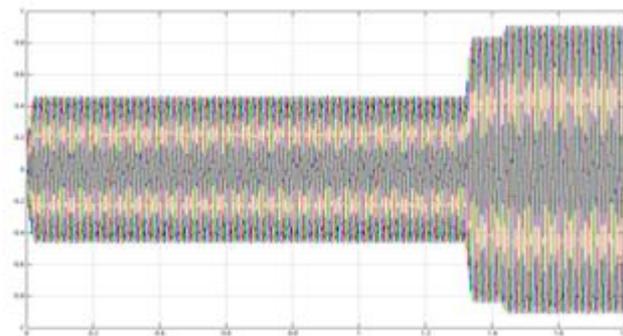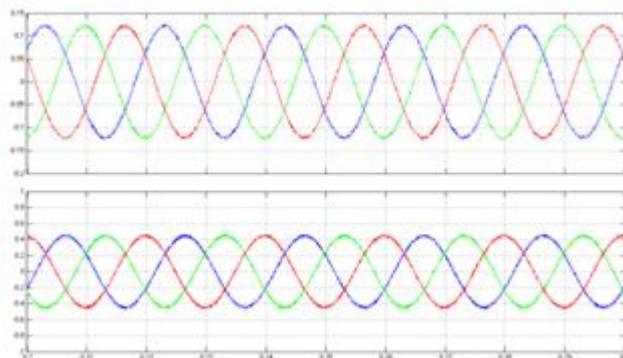

Figure 11: Line Currents for a P and Q Step Change

Figure 12: Line Currents (i_A,i_B, i_C) and Input Matrix Converter Currents(i_a, i_b, i_c) pu

The results of Figure 12. Show line and input matrix converter currents in steady state, for ΔP_{ref}=0.4 p.u.i.e. P_{ref}=0.8p.u., and Q_{ref}=0.4p.u., ΔQ_{ref}=0.2p.u., and Q_{iref}=-0.07p.u.Currents are almost sinusoidal with small ripple content.

CONCLUSIONS

This paper derived advanced non linear direct power controllers, for matrix converters connected to power transmission lines as UPFCs. Presented simulation results show that active and reactive flow will be advantageously controlled by using the proposed DPC. Results show no steady-state errors, no cross coupling, insensitivity to non-modeled dynamics and fast response times, thus confirming the expected performance of the presented nonlinear DPC methodology. Despite showing a suitable dynamic response, the PI performance is inferior when compared to DPC. Furthermore, the PI controllers and modulator take longer times to compute. Obtained results show that DPC is a strong non linear control candidate for line active and reactive power flow.

REFERENCES

1. N. Hingorani and L. Gyugyi, *Understanding FACTS—Concepts and Technology of Flexible AC Transmission Systems*. Piscataway, NJ: IEEE Press/Wiley, 2000.

2. X. Jiang, X. Fang, J. Chow, A. Edris, E. Uzunovic, M. Parisi, and L. Hopkins, "A novel approach for modeling voltage-sourced converterbased FACTS controllers," *IEEE Trans. Power Del.*, vol. 23, no. 4, pp. 2591–2598, Oct. 2008

3. L. Gyugyi, C. Schauder, S. Williams, T. Rietman, D. Torgerson, and A. Edris, "The unified power flow controller: A new approach to power transmission control," *IEEE Trans. Power Del.*, vol. 10, no. 2, pp. 1085–1097, Apr. 1995.

4. C. Schauder, L. Gyugyi, M. Lund, D. Hamai, T. Rietman, D. Torgerson, and A. Edris, "Operation of the unified power flow controller (UPFC) under practical constraints," *IEEE Trans. Power Del.*, vol. 13, no. 2, pp. 630–639, Apr. 1998.

5. T. Ma, "P-Q decoupled control schemes using fuzzy neural networks for the unified power flow controller," in *Electr. Power Energy Syst.*. New York: Elsevier, Dec. 2007, vol. 29, pp. 748–748.

6. L. Liu, P. Zhu, Y. Kang, and J. Chen, "Power-flow control performance analysis of a unified power-flow controller in a novel control scheme," *IEEE Trans. Power Del.*, vol. 22, no. 3, pp. 1613–1619, Jul. 2007.

7. F. Gao and M. Iravani, "Dynamic model of a space vector modulated matrix converter," *IEEE Trans. Power Del.*, vol. 22, no. 3, pp. 1696–1750, Jul. 2007.

8. B. Geethalakshmi and P. Dananjayan, "Investigation of performance of UPFC without DC link capacitor," in *Elect. Power Energy Res.*. New York: Elsevier, 2008, pp. 284–294, 736-746.

9. L. Gyugyi, "Unified power flow control concept for flexible AC transmission systems," *Proc. Inst. Elect. Eng. C*, vol. 139, no. 4, Jul. 1992.

10. R. Strzelecki, A. Noculak, H. Tunia, and K. Sozanski, "UPFC with matrix converter," presented at the EPE Conf., Graz, Austria, Sep. 2001.

11. J. Monteiro, J. Silva, S. Pinto, and J. Palma, "Unified power flow controllers without DC bus: Designing controllers for the matrix converter solution," presented at the Int. Conf. Electrical Engineering, Coimbra, Portugal, 2005.

12. A. Dasgupta, P. Tripathy, and P. Sensarma, "Matrix converter as UPFC for transmission line compensation," in *Proc. 7th Int. Conf. Power Electronics*, Exco, Daegu, Korea, Oct. 2007, pp. 1050–1055.

13. S. Pinto, "Conversores matriciais trifásicos: generalização do commando vectorial directo," Ph.D. dissertation, Instituto Superior Técnico Universidade Técnica de Lisboa, Lisbon, Portugal, Jul. 2003.

14. S. Vazquez, M. Carrasco, J. Leon, and E. Galvan, "A model-based direct power control for three-phase power converters," *IEEE Trans. Ind. Electron.*, vol. 49, no. 2, pp. 276–288, Apr. 2002.

15. M. Malinowski, M. Jasin'ski, and M. Kazmierkowski, "Simple direct power control of three-phase PWM rectifier using space-vector modulation (DPC-SVM)," *IEEE Trans. Ind. Electron.*, vol. 51, no. 2, pp. 447–454, Apr. 2004.

16. G. Zhoua, B. Wub, and D. Xuc, "Direct power control of a multilevel inverter based active power filter," in *Elect. Power Energy Res*. New York: Elsevier, 2007, vol. 77, pp. 284–294.

17. P. Antoniewicz and M. Kazmierkowski, "Virtual-flux-based predictive direct power control of AC/DC converters with online inductance estimation," *IEEE Trans. Ind. Electron.*, vol. 55, no. 12, pp. 4381–4390,Dec. 2008.

18. W. S. Levine*, The Control Handbook*. Boca Raton, FL: CRC, 1996, pp. 911–912.

19. J. Hung, W. Gao, and J. Hung, "Variable structure control: A Survey," *IEEE Trans. Ind. Electron.*, vol. 40, no. 1, pp. 2–22, Feb. 1993.

20. J. F. Silva, "Sliding-mode control of boost-type unity-power-factor PWM rectifiers," *IEEE Trans. Ind. Electron.*, vol. 46, no. 3, pp. 594–603, Jun. 1999.

21. S. Pinto and J. Silva, "Sliding mode direct control of matrix converters," *Inst. Eng. Technol. Elect. Power Appl.*, vol. 1, no. 3, pp. 439–448, 2007.

22. J. Silva and S. Pinto, , M. H. Rashid, Ed., "Power Electronics Handbook," in *Control Methods for Switching Power Converters*, 2nd ed. New York: Academic Press/ Elsevier, 2007, ch. 34, pp. 935–998.